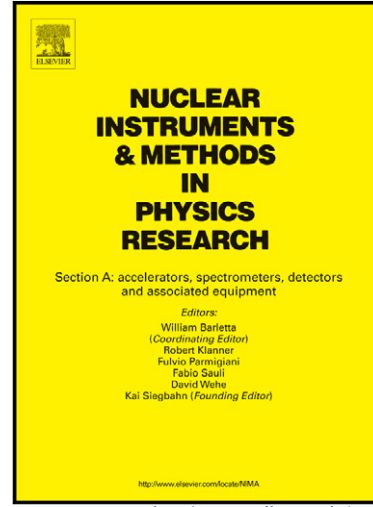


# Author's Accepted Manuscript

Recent developments in photodetection for medical applications

G. Llosá



PII: S0168-9002(15)00104-7

DOI: <http://dx.doi.org/10.1016/j.nima.2015.01.071>

Reference: NIMA57468

To appear in: *Nuclear Instruments and Methods in Physics Research A*

Cite this article as: G. Llosá, Recent developments in photodetection for medical applications, *Nuclear Instruments and Methods in Physics Research A*, <http://dx.doi.org/10.1016/j.nima.2015.01.071>

This is a PDF file of an unedited manuscript that has been accepted for publication. As a service to our customers we are providing this early version of the manuscript. The manuscript will undergo copyediting, typesetting, and review of the resulting galley proof before it is published in its final citable form. Please note that during the production process errors may be discovered which could affect the content, and all legal disclaimers that apply to the journal pertain.

# Recent developments in photodetection for medical applications

G. Llosá<sup>a,\*</sup>

<sup>a</sup>Instituto de Física Corpuscular, CSIC / UVÉG, Valencia, Spain

## Abstract

The use of the most advanced technology in medical imaging results in the development of high performance detectors that can significantly improve the performance of the medical devices employed in hospitals. Scintillator crystals coupled to photodetectors remain to be essential detectors in terms of performance and cost for medical imaging applications in different imaging modalities. Recent advances in photodetectors result in an increase of the performance of the medical scanners. Solid state detectors can provide substantial performance improvement, but are more complex to integrate into clinical detectors due mainly to their higher cost. Solid state photodetectors (APDs, SiPMs) have made new detector concepts possible and have led to improvements in different imaging modalities. Recent advances in detectors for medical imaging are revised.

**Keywords:** detectors, photodetectors, medical applications, PET, SPECT, Hadron Therapy

## 1. Introduction

The use of the most advanced technology in medical imaging results in the development of high performance detectors that can significantly improve the performance of the medical devices employed in hospitals. Scintillator crystals coupled to photodetectors continue to dominate the market in nuclear emission imaging techniques such as Positron Emission Tomography (PET) and Single Photon Emission Computed Tomography (SPECT), given their performance/cost ratio. As in any other application, photodetectors with higher photodetection efficiency are desired, due to the improvement in energy, timing and spatial resolution that this enhancement brings. In addition, in order to make commercial products that can be afforded and employed in hospitals, detectors must be compact, stable and have low cost. In some cases specific characteristics are required, such as compatibility with magnetic fields. Improvements are being obtained with vacuum photodetectors in terms of higher PDE, reduced noise and faster response which can translate into better performance of the medical systems. Also, other options such as solid state detectors can provide substantial performance improvement given their excellent energy and spatial resolution, but are more complex to incorporate to clinical detectors due mainly to their higher cost.

Multicell Geiger-mode Avalanche Photodiodes, also known as silicon photomultipliers (SiPMs) clearly dominate the new developments in nuclear medical imaging, since they are particularly well suited for such applications. They have an increasingly good performance in all aspects at a continuously decreasing cost. Their drawbacks as compared to vacuum photodetectors, such as, for example, higher noise, are not so relevant in applications in which a high amount of light is available. Very

large areas are not necessary and segmented photodetectors are employed. The temperature dependence of their response can be stabilized or compensated for. Their high gain, low operation voltage, compactness and low cost are clear advantages in this field.

SiPMs are employed in several imaging techniques such as PET and SPECT for different applications. For example, their use in intra-operative gamma cameras leads to compact and light imaging devices which can greatly help clinicians. Although the benefits resulting from the improvements in their intrinsic performance are mitigated by the use of collimators, SPECT and gamma cameras are able to detect smaller, deeper and fainter lesions. In PET, SiPMs allow the design of detectors with depth of interaction determination capability to reduce the parallax error. Their insensitivity to magnetic fields, together with a high gain, has made them the photodetector of choice in recent years for the combination of PET and Magnetic Resonance Imaging (MRI). The use of SiPMs has also the potential of significantly improving the performance of PET through time-of-flight techniques.

This paper illustrates some of the recent advances in detectors for nuclear medical imaging and hadron therapy monitoring, in which SiPMs play a dominant role.

## 2. Positron Emission Tomography

Since the development of this technique, PET detectors have undergone major improvements in performance and significant advances are still being achieved.

### 2.1. Depth of Interaction

The PET working principle is based on the simultaneous detection of the two 511 keV photons emitted back to back in the positron annihilation. The two events detected in coincidence are used to determine a volume where the annihilation

\*Corresponding author

Email address: gabriela.llosa@ific.uv.es (G. Llosá)

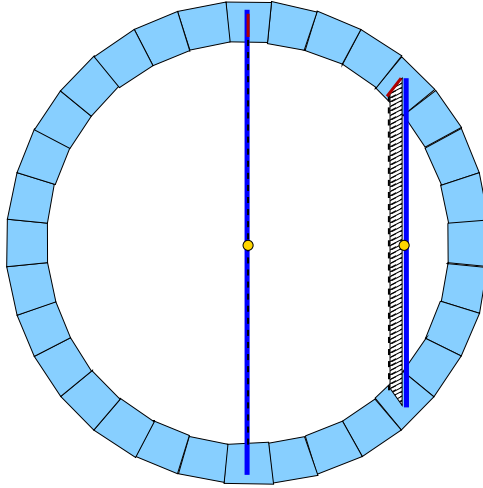


Figure 1: Parallax error. The real LOR (solid line) differs from the one assigned (dashed line) due to the lack of DOI information. The uncertainty grows<sup>99</sup> towards the edges of the FOV.

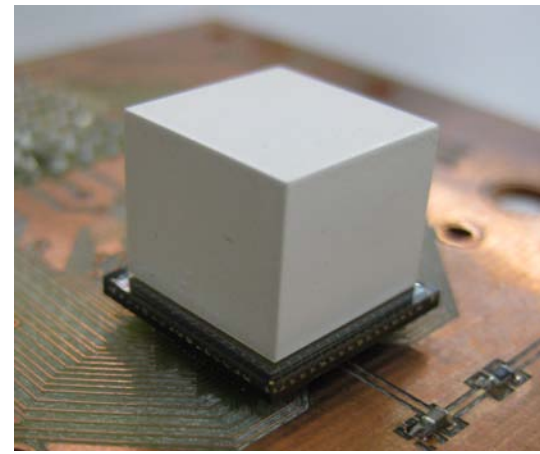


Figure 2: Monolithic crystal of size  $12 \times 12 \times 10 \text{ mm}^3$  painted white coupled to a 64-pixel SiPM array.

coordinate is determined by the WLS and the individual LYSO layers provide discrete DOI information. Images of young rats with excellent resolution have been achieved.

A different approach is the one followed in X'tal cube [4], where an LYSO scintillator block is segmented by laser processing to 3D squares of  $1 \text{ mm}^3$ . Arrays of  $4 \times 4$  SiPMs are optically coupled to each surface of the crystal block. The first imaging tests with this detector have been carried out with successful results.

In contrast to such highly pixellated detectors, renewed interest in continuous crystals has also arisen profiting from the high granularity and gain of new photodetectors, and in particular of SiPMs. The use of continuous crystals can potentially offer high efficiency and excellent spatial resolution. However, accurate positioning algorithms including DOI determination are required to correctly determine the interaction position of the photons in the crystal. An example of this type of detectors is a Ce/Ca co-doped LSO monolithic scintillator crystal of size  $24 \times 24 \times 10 \text{ mm}^3$  read out by a digital dSiPM array, with which a spatial resolution of about  $1 \text{ mm FWHM}$  averaged over the entire crystal was obtained [5]. Another example is a  $12 \times 12 \times 10 \text{ mm}^3$  LYSO continuous white painted crystal coupled to an  $8 \times 8$ -pixel SiPM array with  $1.5 \text{ mm}^2$  pixel pitch (see Fig. 2) with a spatial resolution of  $0.7 \text{ mm FWHM}$  in the center of the crystal [6].

## 2.2. Time-of-Flight-PET

Another area of intense research in PET is the use of Time-of Flight (TOF) techniques to improve the signal-to-noise ratio in the reconstructed images [7]. The LOR restricts the origin of the event to a line connecting the interaction positions of the 511 keV photons in the detectors. However, within the line, all points have equal probability of being the event origin. If the detectors have sufficiently good timing resolution, it is possible to measure the difference in arrival time of the two photons to the two detectors. With perfect timing resolution this would lead to the point along the LOR in which the annihilation took place (if other degradation effects such as acolinearity are ignored). Given the error  $\Delta t$  in the determination of the arrival

time difference and accounting for the propagation of photons at the speed of light  $c$ , it is possible to determine this origin with an error:

$$\Delta x = \frac{c}{2} \Delta t, \quad (1)$$

which restricts the LOR to a segment. This improves the image quality due to a reduction of the statistical noise. Commercial TOF-PET systems have a coincidence time resolution around 500-600 ps FWHM [8], which results in a segment of 7.5-9 cm. The improvement of TOF vs. non-TOF images has been shown both in phantom and patient studies [9].

Time resolution has improved significantly in recent systems. Different types of photodetectors (PMTs, MCPs, SiPMs, dSiPMs) are employed for TOF-PET. Excellent values in the range of 100-200 ps FWHM are obtained with single crystals of different sizes coupled to SiPMs [10], of 200-300 ps FWHM with small detector blocks [11] or also with monolithic crystals [12].

EndoTOFPET-US is a multimodal detector for pancreatic and prostatic cancer. It consists of a PET detector integrated into an endoscopic ultrasound probe and an external plate. Both detectors are composed of arrays of LYSO crystals coupled to SiPMs or dSiPMs. The system aims at a coincidence time resolution better than 200 ps FWHM for the rejection of background from adjacent organs to the one under study. A preliminary design has been developed for both detectors. First tests of the internal probe have been performed with  $0.71 \times 0.71 \times 10 \text{ mm}^3$  LYSO:Ce crystals coupled to SiPMs and a NINO differential amplifier-discriminator, showing an average time resolution of  $187 \pm 27 \text{ ps}$ . The combination with the external plate achieves a coincidence time resolution of  $212 \pm 22 \text{ ps}$  [13].

Full systems with improved timing resolution have also been constructed. A PET ring with a coincidence timing resolution of  $314 \text{ ps} \pm 20 \text{ ps}$  has been developed. The detector modules are composed by  $6.1 \times 6.1 \times 25 \text{ mm}^3$  LSO scintillator crystals coupled on their long side to a 1-inch diameter PMT with super-bialkali photocathode optimized for timing resolution [14]. Images of NEMA phantoms show a very significant visual improvement of TOF versus non-TOF images and a signal-to-noise ratio improvement by a factor of 2.3.

### 2.3. PET-MR

The combination of images of the same object obtained with different imaging modalities (multimodality) has shown to have increased diagnostic value with respect to one modality only. In particular, the combination of a structural imaging modality (eg. Computed Tomography - CT) with a functional modality (eg. PET), provides an anatomical reference to functional images that is of high interest for the clinicians. PET-CT is now the standard in hospitals and PET-only images tend to be no longer acquired.

MR has some advantages over CT: it provides better resolution and soft tissue contrast and it avoids the radiation dose given by CT [15]. However, the combination of PET and MR imaging modalities is difficult given that the performance of PMTs is degraded in magnetic fields.

Initial PET-MR systems were based on optical guides to convey the light from the scintillator outside the magnet where the PMTs can work [16], or used avalanche photodiodes (APDs) as photodetectors [17]. Recent systems are based on SiPMs. A preclinical PET/RF insert for clinical MRI scanner has been developed for simultaneous PET/MR data acquisition. The system has been tested with phantoms, showing low disturbance of the PET and MR systems on each other. A living rat has also been imaged proving the system's in vivo capabilities [18]. Initial tests with dSiPMs are also being carried out in this field [19].

### 3. Intra-operative probes and gamma cameras

Recent developments in gamma cameras include for example the use of solid state detectors [20], new scintillators such as LaBr<sub>3</sub> [21] or new photodetectors such as dSiPMs [22]. The use of SiPMs contributes to the development of compact and light devices. An application in which they are employed is the development of intra-operative devices.

Intra-operative imaging of tumours helps the surgeon to determine precisely the tumour extension and separate it from healthy tissue. A typical application of such devices is the detection of sentinel lymph nodes. This technique relies on the knowledge clinicians have on the way some types of cancer progress (e.g. breast cancer), spreading first to the lymph nodes closest to the primary tumour region. The sentinel lymph node technique consists on determining if the cancer has spread to the lymph node closest to the tumour. If the sentinel lymph node has no cancer, it is likely that the cancer has not spread to other parts of the body. Beta and gamma intra-operative probes in photon counting mode and mini gamma cameras which allow imaging are used for this application. However, these devices in general have small FOV.

In order to image the whole region, devices with larger (around  $4 \times 4 \text{ cm}$  FOV) are necessary, together with excellent spatial resolution while being portable and small. Recently, imaging intra-operative probes with solid state detectors [20] or scintillator detectors coupled to SiPMs are being developed to ensure a precise localization and complete surgical excision of tumors. An example of the use of SiPMs is the SIPMED prototype of a very compact intra-operative gamma camera. It is based on an LYSO scintillator coupled to four monolithic SiPM arrays and dedicated readout electronics, with a FOV of  $5 \times 5 \text{ cm}^2$  [23]. Another example is a LaBr<sub>3</sub> based camera coupled to an array of 80 SiPMs, a circular FOV of 60 mm diameter and a weight of 1.4 kg. The camera has an intrinsic spatial resolution of 4.2 mm FWHM, an energy resolution of 21.1% FWHM at 140 keV, and a sensitivity of 481 and 73 cps/MBq when using single- and double-layer parallel-hole collimators, respectively. It has also been evaluated in the operating room during a human study of melanoma [24].

### 4. Hadron Therapy

Hadron Therapy (HT) is a novel technique that can offer significant benefits over conventional radiation therapies [25].

Conventional radiotherapy employs photons which deposit a higher radiation dose close to the skin decreasing exponentially towards the inner tissue where the tumours are generally located. Charged massive particles such as protons or carbon ions deposit most of the energy at a given depth, according to the Bragg curve. Thus, thanks to the highly conformal dose deposition of charged particles as compared to photons, the dose reaching healthy tissue and organs at risk can be significantly reduced. This fact, together with the higher relative biological effectiveness of charged particles results in superior therapeutic capabilities, in particular for eye tumours, paediatric oncology, radio-resistant tumours or tumours close to critical organs. Given its potential benefits, the number of HT centers in the world is rapidly growing.

However, contrary to radiotherapy in which the therapeutic radiation dose administered to the patient can be directly measured, HT still lacks an accurate method capable of assessing treatment in real time.

The interaction of the therapeutic beam with the tissue during treatment results in the emission of secondary particles (positrons, gamma-rays, nuclear fragments...), which is correlated to the dose deposition. Thus, such particles can be employed as a monitoring agents.

PET is the only technique currently applied for obtaining an independent assessment of the dose delivery. The distribution of positron emitters generated during irradiation (mostly  $^{11}\text{C}$ , half life 20.4 min,  $^{15}\text{O}$ , half life 2.0 min) can be obtained with PET systems [26, 27, 28]. The activity distribution of positron emitters correlates with the dose distribution, but due to the fact that they are different physical processes, a direct evaluation of the dose delivery is not possible. An indirect verification is carried out by comparing the acquired PET images with the corresponding  $\beta^+$  activation pattern deduced from the planned treatment and obtained from detailed Monte-Carlo simulations. However this method has important limitations such as the very low  $\beta^+$  activity induced during irradiation, the relatively long nuclear lifetimes and the fraction of activity carried away from the production location due to physiological processes (biological washout) [29].

The improvement of PET detectors for treatment monitoring is mainly being done through the development of TOF-PET systems to minimize the effect of the scanner gaps in the reconstructed images, by ensuring a fast transfer from the treatment gantry to a nearby PET system or by developing accurate models of biological washout [30].

As an alternative to PET, different dose monitoring methods are under study and being developed, most of them aimed at using prompt gammas that are generated during the treatment due to the excitation of the tissue nuclei. Gammas are produced in a larger amount and shorter (ns) times after irradiation than positron emitters. Collimated gamma cameras [31] or Compton cameras with different types of detectors and configurations including CZT detectors [32], silicon detectors [33] or scintillator detectors [34] are being evaluated to assess their possible use as monitoring devices.

Collimated gamma cameras provide a practical alternative which is showing good results. A system under test is com-

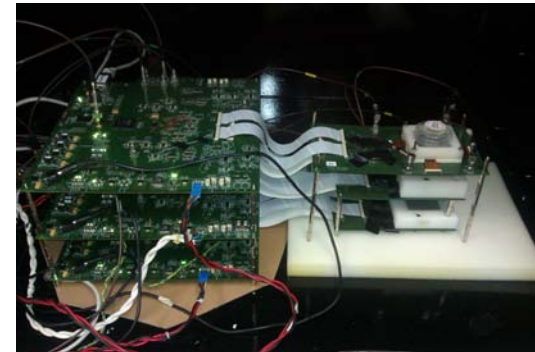


Figure 3: Compton telescope composed of three layers of  $\text{LaBr}_3$  crystals coupled to SiPM arrays and readout electronics.

posed of an LYSO scintillator detector with a 100 mm deep tungsten collimator with a single, 4 mm wide parallel-edge slit. The system has been tested with 160 MeV protons impinging a movable PMMA target. TOF techniques were employed to reduce the background due to neutrons. The study shows that the position of the falloff and entrance rise of prompt-gamma emission can be seen qualitatively, and also can be measured quantitatively by comparison with a reference profile [35].

A Compton camera is being developed consisting of two scatter planes, two CdZnTe (CZT) cross strip detectors, and an absorber consisting of one LSO block detector. Images have been acquired in the laboratory. In addition, tests in a linear electron accelerator which produces bunched bremsstrahlung photons with up to 12.5 MeV energy show that the detector setup is suitable for time-resolved background discrimination in realistic radiation environments corresponding to pulsed clinical particle accelerators [36].

Another alternative consists of a  $\text{LaBr}_3$  Compton telescope composed of three scintillator layers coupled to SiPM arrays [37] (see Fig. 3). A dedicated image reconstruction method has also been developed. The device has been tested in the laboratory with a  $^{22}\text{Na}$  source, and it is capable of reconstructing successfully the source position.

Also related to hadron therapy, the development of primary beam monitoring hodoscopes is essential for quality assurance of the beam, to ensure a precise knowledge of its profile and characteristics. In addition, the information can be used to assist the treatment monitoring imaging devices. An hodoscope should have a count rate capability of  $10^8$  pps, with an accuracy of 1 ns. Different alternatives are being developed, based for example on gaseous detectors or on scintillating fibers. An example of such a system constructed with scintillating fibers consists of an array of  $2 \times 128$  scintillating fibers of  $1\text{ mm} \times 1\text{ mm}$  size coupled to a multianode PMT which has successfully imaged proton and Carbon ion beam profiles [38].

## 5. Conclusions

Significant advances are being made in different areas of medical imaging that contribute to a better diagnosis, control of the treatment or evaluation of the evolution of the disease.

339 The use of new detectors and the transfer of knowledge from 402  
 340 other fields can greatly contribute to this aim. Solid state detec- 403  
 341 tors provide performance enhancement of the systems, but the 404  
 342 performance/cost ratio of scintillator-photodetector systems, to- 405  
 343 gether with their improvements, makes them still the dominant 406  
 344 detectors in this field. In particular, the introduction of SiPMs 408  
 345 in medical imaging applications has benefitted some research 409  
 346 areas such as TOF-PET, the combination of PET and MRI or the 410  
 347 design of detectors with DOI determination. In SPECT and 412  
 348 gamma cameras, the use of improved detectors allows to detect 413  
 349 smaller, deeper and fainter lesions, and to design compact and 414  
 350 portable intra-operative devices. Also, new techniques, such 416  
 351 as the application of collimated and Compton cameras to dose 417  
 352 monitoring in hadron therapy have arisen in recent years as an 418  
 353 important field of research.

## 354 Acknowledgments

355 The author's research was supported in part by the Eu- 425  
 356 ropean Commission's 7th Framework Programme through a 426  
 357 Marie Curie European Reintegration Grant (ASPID GA NUM 427  
 358 239362) and the ENVISION project (G. A. num 241851), 428  
 359 by the Spanish *Ministerio de Economía y Competitividad* 429  
 360 (FPA2010-14891 and FIS2011-14585-E), the Universitat de 431  
 361 Valéncia (UV-INV-PRECOMP12-80755) and the Generalitat 432  
 362 Valenciana (GV/2013/133). The author is supported through a 433  
 363 JAE-DOC fellowship, co-funded by the Fondo Social Europeo. 434  
 364 [1] D. Renker. Geiger-mode avalanche photodiodes, history, properties and 435  
 365 problems. *nucl. Instr. Meth. A*. Vol 567 (1), 2006, p 4856.

366 [2] M.V. Green et al. Experimental Evaluation of Depth-of-Interaction Cor- 437  
 367 rection in a Small-Animal Positron Emission Tomography Scanner. *Mol* 438  
 368 *Imaging*. 2010 ; 9(6): 311-318.

369 [3] E. Bolle et a. The AX-PET experiment: A demonstrator for an axial 440  
 370 Positron Emission Tomograph. *Nucl. Inst. Meth. Phys. Res. Sec. A*, 2013, 441  
 371 volume 718, pages 126 - 129, number 0.

372 [4] E. Yoshida et al. Impact of Laser-Processed X'tal Cube Detectors on PET 444  
 373 Imaging in a One-Pair Prototype System. *IEEE Trans. Nucl. Sci.* Vol 60 I<sub>445</sub>  
 374 5 (2013) 3172 - 3180.

375 [5] S. Seifert et al. First characterization of a digital SiPM based time-of- 446  
 376 flight PET detector with 1 mm spatial resolution. *Phys. Med. Biol.* 58<sub>447</sub>  
 377 (2013) 3061.

378 [6] J. Cabello et al. High resolution detectors based on continuous crystals<sub>450</sub>  
 379 and SiPMs for small animal PET. *Nucl. Inst. Meth. A*, 2013, volume 718,<sub>451</sub>  
 380 pages 148 - 150.

381 [7] W. W. Moses. Time of Flight in PET Revisited. *IEEE Trans. Nucl. Sci.* 452  
 382 vol 50, no5, (2013) 1325-1330.

383 [8] Surti S, Kuhn A, Werner ME, Perkins AE, Kolthammer J, Karp JS. Perfor- 453  
 384 mance of Philips Gemini TF PET/CT scanner with special considera- 454  
 385 tion for its time-of-flight imaging capabilities. *J Nucl Med*. 2007; 48(3):471- 455  
 386 480.

387 [9] Karp JS, Surti S, Daube-Witherspoon ME, Muehllehner G. Benefit of 456  
 388 Time-of-Flight in PET: Experimental and Clinical Results. *J Nucl Med* 460  
 389 2008; 49(3):462-470

390 [10] S. Gundacker et al. Time of flight positron emission tomography towards 461  
 391 100 ps resolution with L(Y)SO: an experimental and theoretical analysis.<sub>462</sub>  
 392 2013 JINST 8 P07014.

393 [11] C. Casella, M. Heller, C. Joram, T. Schneider. A high resolution TOF- 463  
 394 PET concept with axial geometry and digital SiPM readout. *Nucl. Instr.* 465  
 395 *Meth. A* 736(2014)161-168.

396 [12] H.T. van Dam, G. Borghi, S. Seifert, and D.R. Schaart. Sub-200 ps CRT 466  
 397 in monolithic scintillator PET detectors using digital SiPM arrays and 467  
 398 maximum likelihood interaction time estimation. *Phys. Med. Biol.* 58,<sub>468</sub>  
 399 3243-3257, 2013.

400 [13] N. Aubry et al. EndoTOFPET-US: a novel multimodal tool for endoscopy 470  
 401 and positron emission tomography. 2013 JINST 8 C04002.

- [14] Q. Peng et al. Imaging performance of the Tachyon Time-of-Flight PET camera. 2013 IEEE NSS MIC conference record.
- [15] A. Boss. Hybrid PET/MRI of Intracranial Masses: Initial Experiences and Comparison to PET/CT. *J. Nucl. Med.* 2010;51:1198-1205.
- [16] R.C. Hawkes et al. Preliminary Evaluation of a combined microPET-MR system. *Technology in Cancer Research and Treatment*. Vol. 9, Num 1, 2010, 53-60.
- [17] B.J. Pichler et al. Performance test of an LSO-APD detector in a 7-T MRI scanner for simultaneous PET/MRI. *J Nucl Med*. 2006; 47(4):639-47.
- [18] B. Weissler et al. MR compatibility aspects of a silicon photomultiplier-based PET/RF insert with integrated digitisation. *Phys. Med. Biol.* 59 (2014) 5119.
- [19] J. Wehner. PET/MRI insert using digital SiPMs: Investigation of MR-compatibility. *Nucl. Instr. Meth. A*, Vol 734 (2014), p 116121.
- [20] C. Robert et al. Optimization of a parallel hole collimator/CdZnTe gamma-camera architecture for scintimammography. *Med Phys.* 2011 Apr;38(4):1806-19.
- [21] R. Pani et al. Investigation on a small FoV gamma camera based on LaBr<sub>3</sub>:Ce continuous crystal. *Nucl. Phys. B* 197 (2009), p 202205.
- [22] C. Bouckaert et al. Optimization of digital silicon photomultipliers for monolithic SPECT scintillators. *J Nucl Med.* 2013; 54 (Supp. 2):2160.
- [23] T. A. Imando et al. Miniaturized multi-channels SiPM read-out electronics for medical imaging application. *Proceedings of Science*.
- [24] K. Popovic et al. Development and characterization of a round hand-held silicon photomultiplier based gamma camera for intraoperative imaging. *IEEE Trans. Nucl. Sci.* Vol. 61 Num.3 2014, p 1804.
- [25] D. Cussol. Nuclear Physics and hadrontherapy. Application of Nuclear techniques: Eleventh International Conference. AIP Conference Proceedings, Volume 1412, pp. 303-310 (2011).
- [26] K. Parodi et al. Patient study on in-vivo verification of beam delivery and range using PET/CT imaging after proton therapy. *Int. J. Radiat. Oncol. Biol. Phys.* 68 920-34.
- [27] F. Fiedler et al. On the effectiveness of ion range determination from in-beam PET data. *Phys. Med. Biol.* 55 (2010) 1989-1998.
- [28] S. Combs et al., Monitoring of patients treated with particle therapy using positron emission tomography (PET): the MIRANDA study. Study protocol. *BMC Cancer* 2012, 12:133.
- [29] F. Le Foullher et al., Monte Carlo simulations of prompt-gamma emission During Carbon Ion Irradiation. *IEEE Trans. Nuc. Sci.*, Vol 57, No 5, 2010. 2768-2772.
- [30] X. Zhu, G. El Fakhri. Proton Therapy Verification with PET Imaging. *Theranostics*.2013; 3(10):731-740.
- [31] C. H. Min et al. Prompt gamma measurements for locating the dose falloff region in the proton therapy. *Appl. Phys. Lett.* 89 183517, 2006.
- [32] T. Kormoll et al., A Compton imager for in-vivo dosimetry of proton beams - A design study. *Nucl. Instrum. Meth. A* 114 (2011) 626-627.
- [33] M.-H. Richard et al., Design Guidelines for a Double Scattering Compton Camera for Prompt-g Imaging During Ion Beam Therapy: A Monte Carlo Simulation Study. *IEEE Trans. Nucl. Sci.*, 1:87-94, 2011.
- [34] G. Llosá et al. First Compton telescope prototype based on continuous LaBr<sub>3</sub>-SiPM detectors. *Nucl. Inst. Meth. A*,718(2013)130-133.
- [35] F. Roellinghoff et al. Real-time proton beam range monitoring by means of prompt-gamma detection with a collimated camera. *Phys. Med. Biol.*, 59 (2014) 1327-1338.
- [36] F. Hueso-Gonzalez. Test of Compton camera components for prompt gamma imaging at the ELBE bremsstrahlung beam. 2014 JINST 9 P05002.
- [37] M. Trovato et al. A three layer Compton telescope for dose monitoring in hadron therapy. 2013 IEEE NSS MIC Conf. Rec. M07-4.
- [38] J. Krimmer et al. Real-time monitoring of the ion range during hadron-therapy: An update on the beam tagging hodoscope. ICTR-PHE 2014. Geneva, Switzerland.